Supporting Information

Triplet-triplet energy transfer from Bi^{3+} to Sb^{3+} in zero-dimensional indium hybrids via B-site co-doping strategy toward white-light emission

Qiqiong Ren,[a] Jian Zhang,[a] Maxim S. Molokeev,[b,c,d] Guojun Zhou*[a] and Xian-Ming Zhang*[a,e]

a Key Laboratory of Magnetic Molecules and Magnetic Information Materials (Ministry of Education), School of Chemistry and Material Science, Shanxi Normal University, Taiyuan 030031, China.

b Laboratory of Crystal Physics, Kirensky Institute of Physics, Federal Research Center KSC SB RAS, Krasnoyarsk 660036, Russia.

c Research and Development Department, Kemerovo State University, Kemerovo, 650000, Russia.

d Department of Physics, Far Eastern State Transport University, Khabarovsk 680021, Russia.

e College of Chemistry & Chemical Engineering, Key Laboratory of Interface Science and Engineering in Advanced Material, Ministry of Education, Taiyuan University of Technology, Taiyuan, Shanxi 030024, P. R. China.

**Corresponding author. Key Laboratory of Magnetic Molecules and Magnetic Information Materials (Ministry of Education), School of Chemistry and Material Science, Shanxi Normal University, Taiyuan 030031, China*

E-mail addresses: zhougj@sxnu.edu.cn (G. J. Zhou), zhangxm@dns.sxnu.edu.cn (X.M. Zhang).

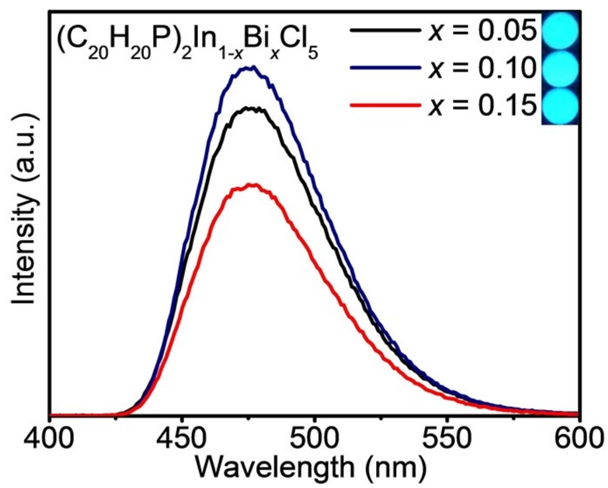

Fig. S1 PL spectra of $(C_{20}H_{20}P)_2In_{1-x}Bi_xCl_5$ (x = 0.05, 0.10, 0.15) excited at 365 nm. Insets show corresponding optical photographs of above compounds excited by 365 nm UV lamp.

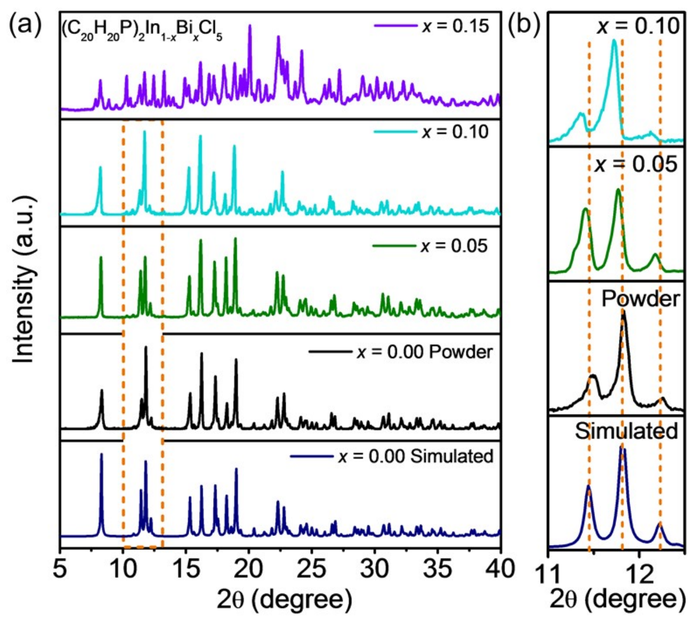

Fig. S2 (a) PXRD patterns of $(C_{20}H_{20}P)_2In_{1-x}Bi_xCl_5$ (x = 0, 0.05, 0.10, 0.15) and standard diffraction pattern of $(C_{20}H_{20}P)_2InCl_5$. (b) Selected diffraction peaks in the range of 11°–12.5° of $(C_{20}H_{20}P)_2In_{1-x}Bi_xCl_5$ (x = 0, 0.05, 0.10).

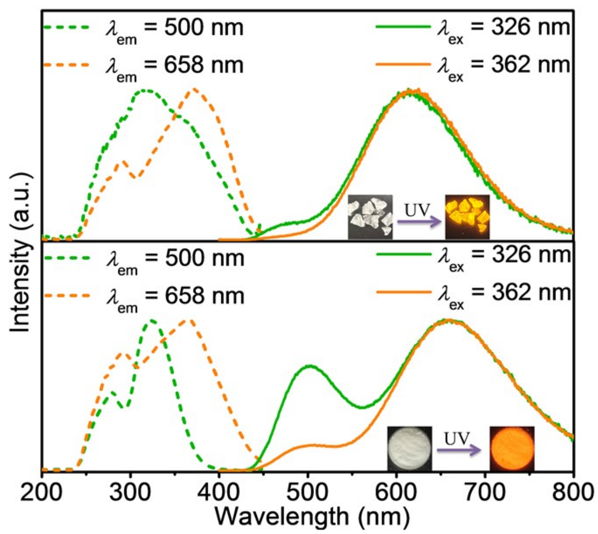

Fig. S3 PLE and PL spectra of single crystal (top) and powder (bottom) samples of $(C_{20}H_{20}P)_2In_{1-x-y}Bi_xSb_yCl_5$ (x = 0, y = 0.10). Insets show the pictures of single crystal (top) and powder (bottom) under daylight and UV excitation.

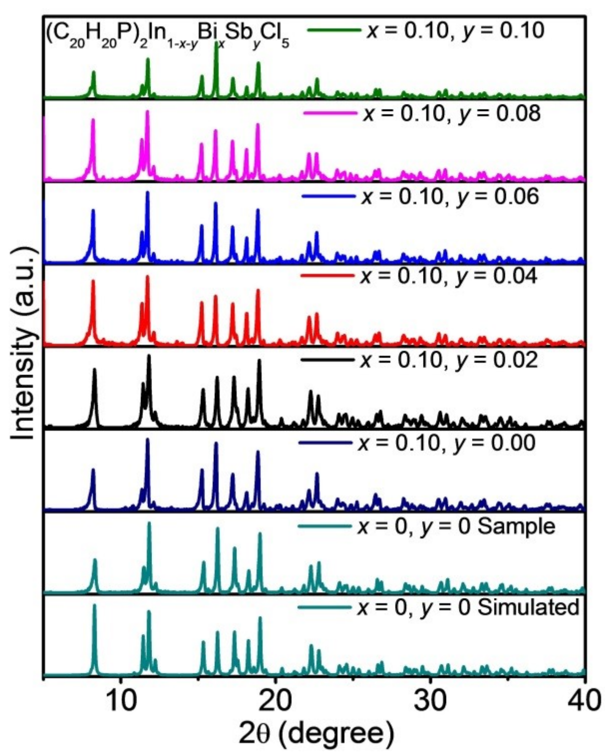

Fig. S4 PXRD patterns of $(C_{20}H_{20}P)_2In_{1-x-y}Bi_xSb_yCl_5$ (x = 0, y = 0) (x = 0.10, y = 0−0.10) and standard diffraction pattern of $(C_{20}H_{20}P)_2InCl_5$.

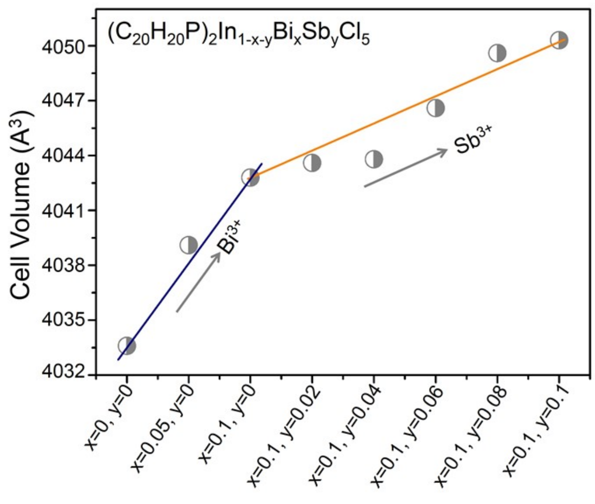

Fig. S5 Variation of unit cell volume with x and y of $(C_{20}H_{20}P)_2In_{1-x-y}Bi_xSb_yCl_5$.

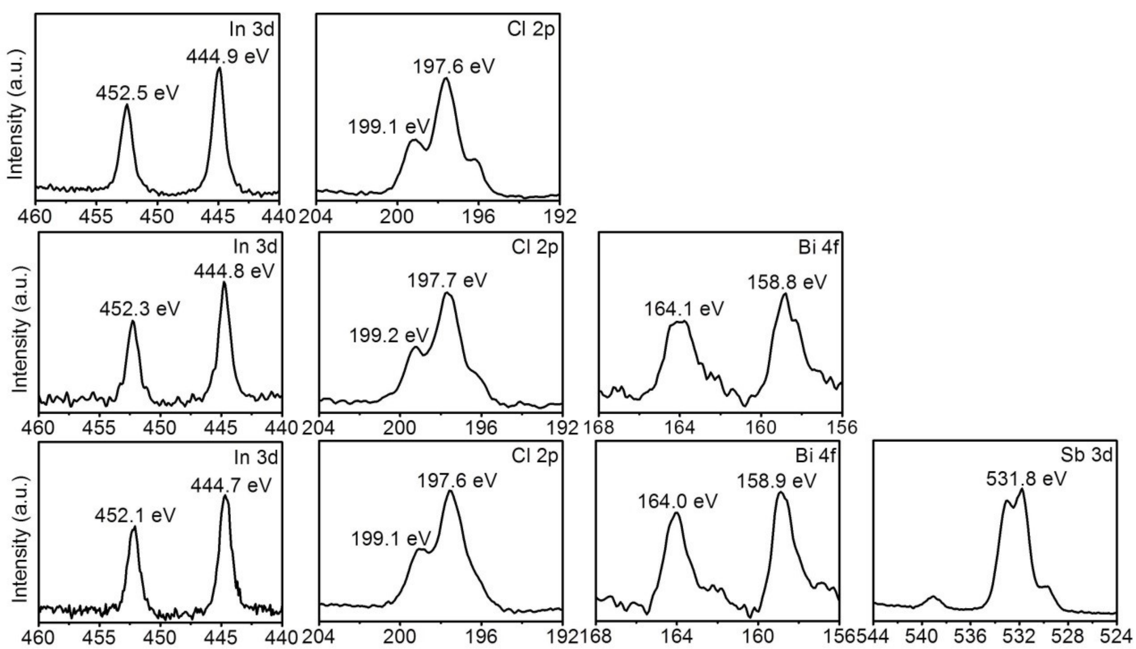

Fig. S6 XPS spectra corresponding to In 3d, Cl 2p, Bi 4f and Sb 3d, respectively, of (a) $(C_{20}H_{20}P)_2InCl_5$, (b) $(C_{20}H_{20}P)_2In_{1-x-y}Bi_xSb_yCl_5$ (x = 0.10, y = 0) and (c) $(C_{20}H_{20}P)_2In_{1-x-y}Bi_xSb_yCl_5$ (x = 0.10, y = 0.10).

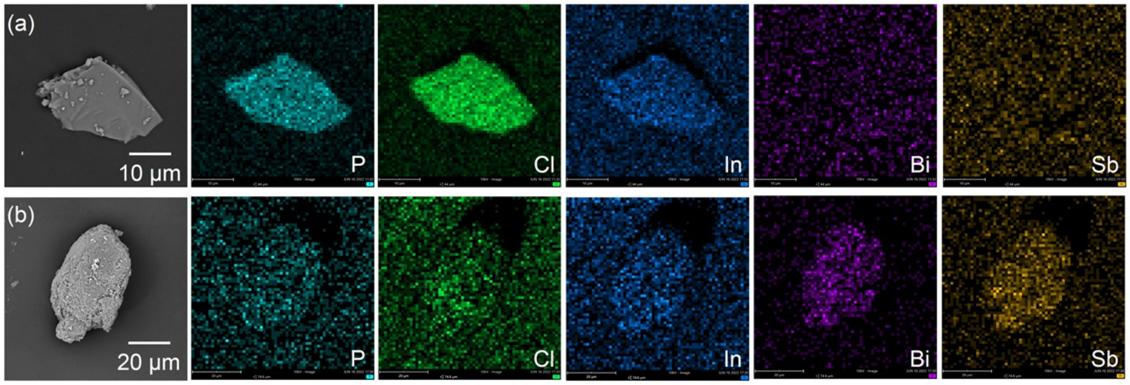

Fig. S7 SEM images and EDS elemental mapping images showing the homogeneous distribution of P, Cl, In, Bi and Sb in different compounds of (a) $(C_{20}H_{20}P)_2InCl_5$ and (b) $(C_{20}H_{20}P)_2In_{1-x-y}Bi_xSb_yCl_5$ (x = 0.10, y = 0.10).

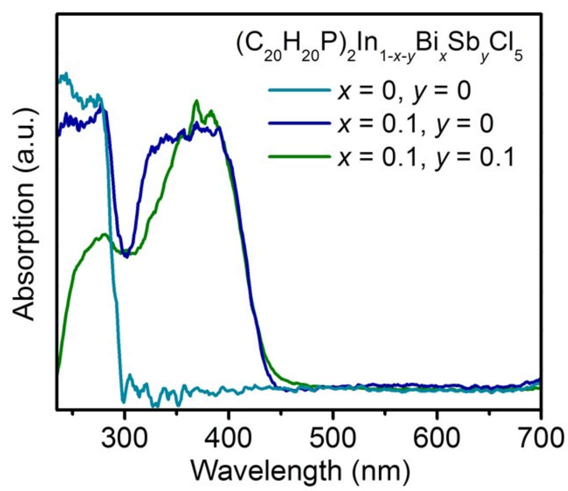

Fig. S8 Absorption spectra of compounds $(C_{20}H_{20}P)_2In_{1-x-y}Bi_xSb_yCl_5$ (x = 0, y = 0) (x = 0.10, y = 0) (x = 0.10, y = 0.10).

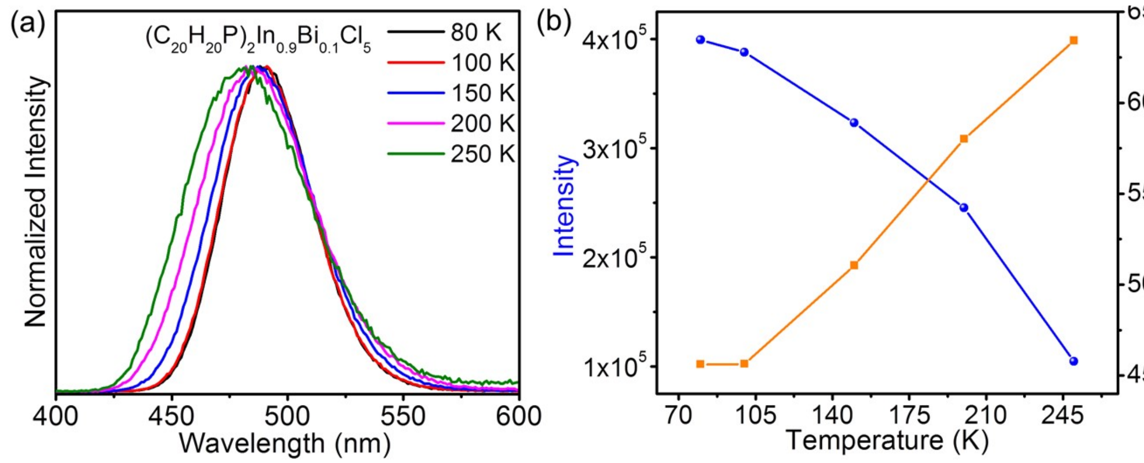

Fig. S9 (a) Normalized temperature-dependent emission spectra of $(C_{20}H_{20}P)_2In_{1-x-y}Bi_xSb_yCl_5$ (x = 0.10, y = 0). (b) Temperature dependence of PL intensity and FWHM.

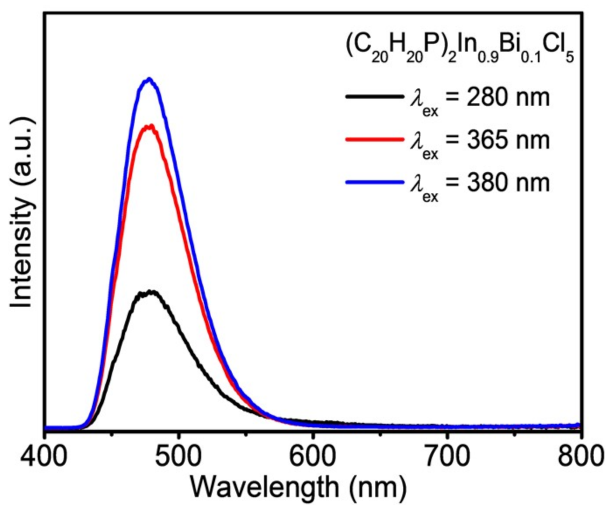

Fig. S10 Emission spectra of $(C_{20}H_{20}P)_2In_{1-x-y}Bi_xSb_yCl_5$ (x = 0.10, y = 0) monitored at different excitation wavelengths.

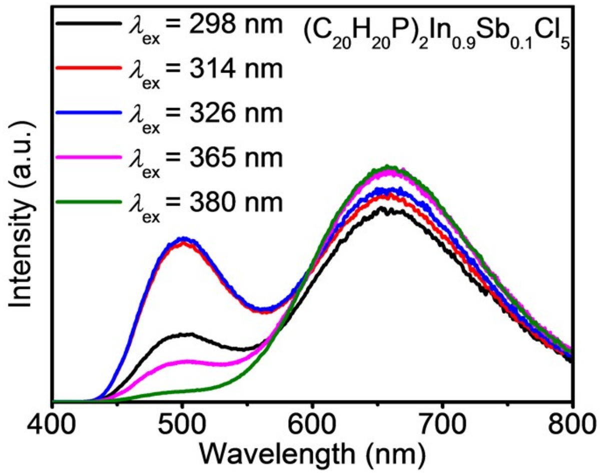

Fig. S11 Excitation-dependent PL spectra of $(C_{20}H_{20}P)_2In_{1-x-y}Bi_xSb_yCl_5$ (x = 0, y = 0.10) with the excitation wavelength ranging from 298 to 380 nm.

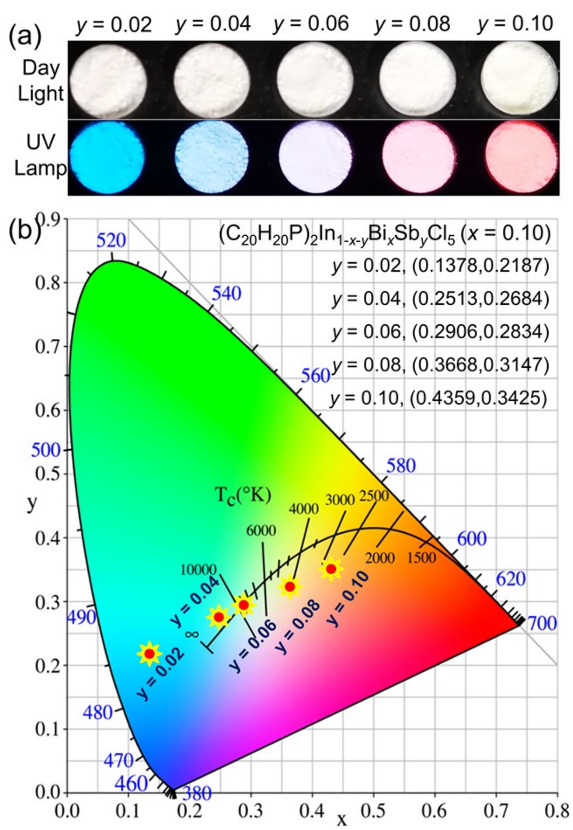

Fig. S12 (a) Photographs of $(C_{20}H_{20}P)_2In_{1-x-y}Bi_xSb_yCl_5$ (x = 0.10, y = 0.02−0.10) under daylight (top) and UV lamp (bottom). (b) The corresponding CIE chromaticity diagrams.

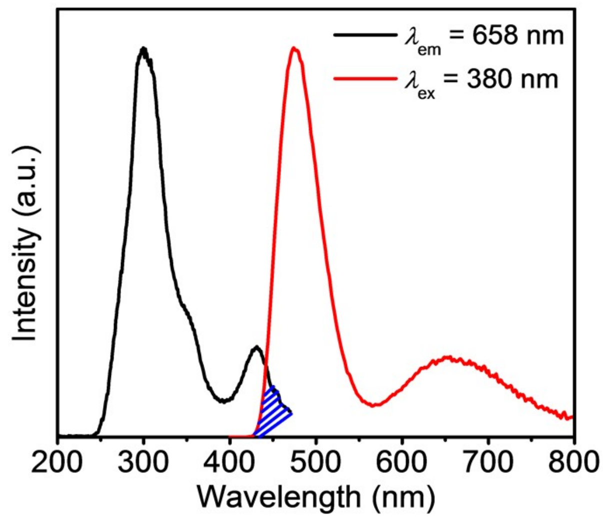

Fig. S13 Normalized PLE and PL spectra of compound $(C_{20}H_{20}P)_2In_{1-x-y}Bi_xSb_yCl_5$ (x = 0.10, y = 0.04). The blue shading represents the intersection.

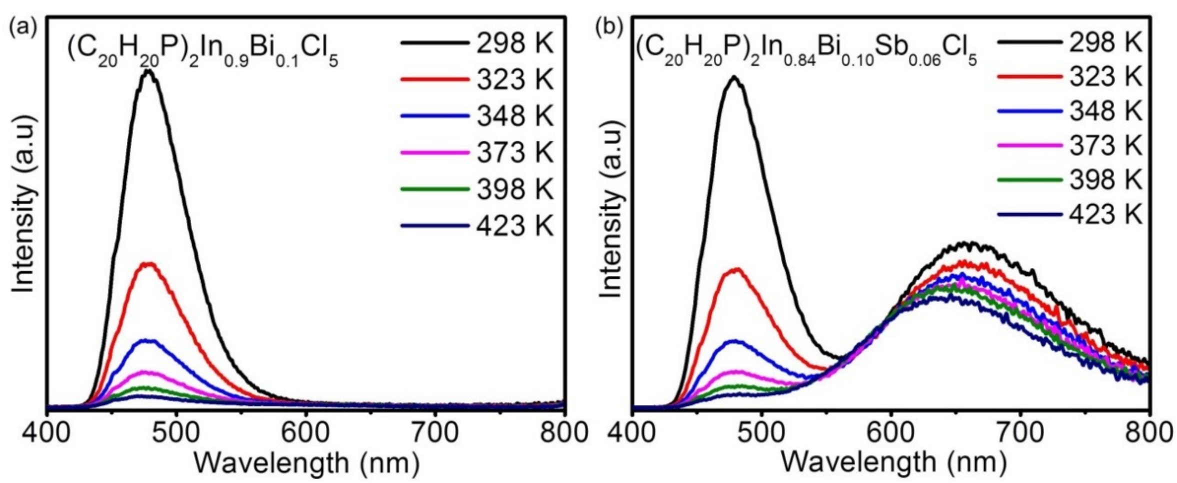

Fig. S14 Temperature-dependent PL spectra of (a) $(C_{20}H_{20}P)_2In_{1-x-y}Bi_xSb_yCl_5$ (x = 0.10, y = 0) and (b) $(C_{20}H_{20}P)_2In_{1-x-y}Bi_xSb_yCl_5$ (x = 0.10, y = 0.06) under 365 nm excitation ranging from 298 K to 423K.

Table S1. Main parameters of processing and refinement of $(C_{20}H_{20}P)_2In_{1-x-y}Bi_xSb_yCl_5$ ($x = 0$, $y = 0$) ($x = 0.10$, $y = 0$) ($x = 0.10$, $y = 0.10$).

Compound	$\mathbf{x = 0, y = 0}$	$\mathbf{x = 0.1, y = 0}$	$\mathbf{x = 0.1, y = 0.1}$
Sp.Gr.	*I*2/*a*	*I*2/*a*	*I*2/*a*
a, Å	17.6594 (5)	17.6602 (9)	17.6770 (8)
b, Å	14.7450 (4)	14.7590 (7)	14.7568 (6)
c, Å	16.7561 (5)	16.777 (1)	16.7904 (8)
β, °	112.414 (2)	112.405 (3)	112.370 (2)
V, Å^3	4033.6 (2)	4042.8 (4)	4050.3 (3)
2θ-interval, °	5-120	5-120	5-120
R_{wp}, %	8.07	9.72	8.17
R_p, %	5.99	7.20	5.73
R_{exp}, %	3.56	3.51	3.60
χ^2	2.26	2.77	2.27
R_B, %	3.35	3.67	2.31

Table S2. ICP-AES results of $(C_{20}H_{20}P)_2In_{1-x-y}Bi_xSb_yCl_5$ ($x = 0$, $y = 0$) ($x = 0.10$, $y = 0$) ($x = 0.10$, $y = 0.10$).

Compound	$\mathbf{(C_{20}H_{20}P)_2InCl_5}$		$\mathbf{(C_{20}H_{20}P)_2In_{0.9}Bi_{0.1}Cl_5}$		$\mathbf{(C_{20}H_{20}P)_2In_{0.8}Bi_{0.1}Sb_{0.1}Cl_5}$	
	Mass%	Atom%	Mass%	Atom%	Mass%	Atom%
In	12.28	0.1070	11.12	0.0968	9.20	0.0801
Bi			1.19	0.0057	1.24	0.0059
Sb					1.01	0.0083

Table S3. Calculated excitation energies and oscillator strengths of $[SbCl_5]^{2-}$ and $[BiCl_5]^{2-}$.

$[SbCl_5]^{2-}$	excitation energies	oscillator strengths	$[BiCl_5]^{2-}$	excitation energies	oscillator strengths
$S_0 \rightarrow S_1$	4.2170 eV	0.1259	$S_0 \rightarrow S_1$	4.5432 eV	0.0737
$S_0 \rightarrow S_2$	4.9471 eV	0.3132	$S_0 \rightarrow S_2$	4.5472 eV	0.0739
$S_0 \rightarrow S_3$	5.4933 eV	0.3826			
$S_0 \rightarrow T_1$	0.6639 eV	0.0003			
$S_0 \rightarrow T_3$	2.0150 eV	0.1525	$S_0 \rightarrow T_3$	1.1200 eV	0.0006
$S_0 \rightarrow T_4$	2.2446 eV	0.0063			
$S_0 \rightarrow T_5$	2.3158 eV	0.0047			